

Supporting Information

Prolonging Exciton Diffusion Length via Manipulating Molecular Stacking Enables Pseudo-Planar Heterojunction Organic Solar Cells Over 19% Efficiency

Ke Wang, Fuwen Zhao, Yufan Zhu, Yi He, Zesheng Liu, Xiao Han, Qi Ai, Xingxing Shen, Bao Li, Jianqi Zhang, Yuze Lin, Chunru Wang and Dan He**

- 1. General characterization**
- 2. Synthesis**
- 3. NMR spectra**
- 4. Absorption**
- 5. Thermogravimetric analysis (TGA)**
- 6. Trap density**
- 7. Grazing-incidence wide-angle X-ray scattering (GIWAXS)**
- 8. Atomic force microscope (AFM)**
- 9. Theoretical calculation**
- 10. Transient absorption (TA)**
- 11. Device fabrication and measurement**
- 12. Space charge limited current (SCLC)**

1. General characterization

^1H NMR, ^{13}C NMR and ^{19}F NMR spectra were measured on a Bruker Avance-400 spectrometer. UV-vis absorption spectra were measured on a UV-2600 UV-vis Spectrophotometer (Shimadzu, Japan). Steady-state photoluminescence (PL) spectra were measured with a Horiba HR Evolution spectrometer at room temperature. We used a 100 lines per millimeter grating. The excitation light was a 532 nm continuous wave laser (3 μW , spot size $\sim 1\ \mu\text{m}$) and was focused onto the sample by a $\times 100$ objective lens (OLYMPUS, NA = 0.9). The photoluminescence quantum yield measurement (PLQY) tests were carried out on a steady-state fluorescence spectrometer FLS-1000. The excitation wavelength is 600 nm and the bandwidth is 8 nm and the emission wavelength is 600 nm with a bandwidth of 3.3 nm and an integration time of 0.5 s. The samples used for PL and PLQY measurements were obtained by spin-coating the solution on the quartz substrate. Fourier-transform photocurrent spectroscopy external quantum efficiency (FTPS-EQE) was performed by an integrated system (PECT-600, Enli Technology Co. Ltd.), where the photocurrent was amplified and modulated by a lock-in instrument. GIWAXS measurements were conducted on an Xenocs-SAXS/WAXS system with an X-ray wavelength of 1.5418 \AA and 0.2° as an incidence angle. Pilatus 300 K was used as a 2D detector. AFM was performed on a Bruker Dimension icon using tapping mode. The J - V curves were measured by using a Keithley 2450 source-measure unit in the nitrogen-filled glove box along the forward scan direction from -0.2 V to 1 V at room temperature. The scan speed and dwell times were fixed at 0.02 V per step and 0 ms, respectively. The photocurrent was measured under AM 1.5G illumination at $100\ \text{mW cm}^{-2}$ by using a 3A solar simulator (LSS-55, JINZHU TECH, calibrated at 02/15/2022). Light intensity was calibrated with a standard photovoltaic cell equipped with a KG2 filter (certificated by the National PV Industry Measurement and Testing Center, 02/15/2022). The EQE measurements of devices were carried out in the air with a solar cell spectral response measurement system (QE-R3018, Enli Technology Co., Ltd). The light intensity at each wavelength was calibrated by a standard single-crystal Si photovoltaic cell. The thickness of all films was measured by the Bruker Dektak-XT. The geometry of complex SA-5F/Y6 was optimized by density functional theory at the B3LYP/6-31G** level, and Grimme's dispersion GD3 and BSSE correction were all considered.

2. Synthesis

Unless stated otherwise, all solvents and chemical reagents were obtained commercially and used without further purification. 2,3,4,5,6-pentafluorobenzaldehyde and pyridine were purchased from Innochem Co. 2-(5,6-difluoro-3-oxo-2,3-dihydro-1*H*-inden-1-ylidene) malononitrile was purchased from HWRK Chem Co. The polymer donors, D18 and PM6, and small molecular acceptors, Y6, BTP-eC9 and L8-BO, were purchased from Derthon Co. and Solarmer Energy Inc., respectively.

SA-5F. 2,3,4,5,6-pentafluorobenzaldehyde (0.16 g, 0.81 mmol) and 2-(5,6-difluoro-3-oxo-2,3-dihydro-1*H*-inden-1-ylidene) malononitrile (0.74 g, 4.1 mmol) were added to a mixture solvent of chloroform (10 mL) and pyridine (0.5 mL). Then the reaction was placed in an oil bath under $65\ ^\circ\text{C}$ and stirred for 48 hours. The mixture was firstly purified by silica gel column chromatography by using dichloromethane as eluent and then recrystallized by petroleum ether to offer the product, SA-5F, as yellow solid (230 mg, yield 80%). ^1H NMR (CDCl_3 , 400 MHz, δ/ppm): 7.94-7.87 (m, 1H), 7.82-7.71 (m, 1H), 7.65 (s, 1H). ^{13}C NMR (CDCl_3 , 100 MHz, δ/ppm): 185.28(s), 184.37(s), 157.22(t), 154.57(q), 146.34(s), 143.99(d), 141.59(s), 140.01(q), 138.93(s), 138.06(q), 136.46(t), 134.25(s), 126.21(s), 112.92(t), 112.75(d), 108.19(q). ^{19}F NMR (CDCl_3 , 376 MHz, δ/ppm): -120.17 (d, $J = 18.5\ \text{Hz}$), -120.54 (d, $J = 18.5\ \text{Hz}$), -134.61 (ddd, $J = 16.4, 12.1, 5.6\ \text{Hz}$), -148.90 (ddd, $J = 21.0, 14.9, 4.5\ \text{Hz}$), -161.19 (m).

SA-0F. The SA-0F was prepared according to the reported literature.^[1] ¹H NMR (CDCl₃, 400 MHz, δ/ppm): 8.46 (d, *J* = 8.0 Hz, 2H), 8.12-7.96 (m, 2H), 7.91 (s, 1H), 7.87-7.75 (m, 2H), 7.64-7.44 (m, 3H).

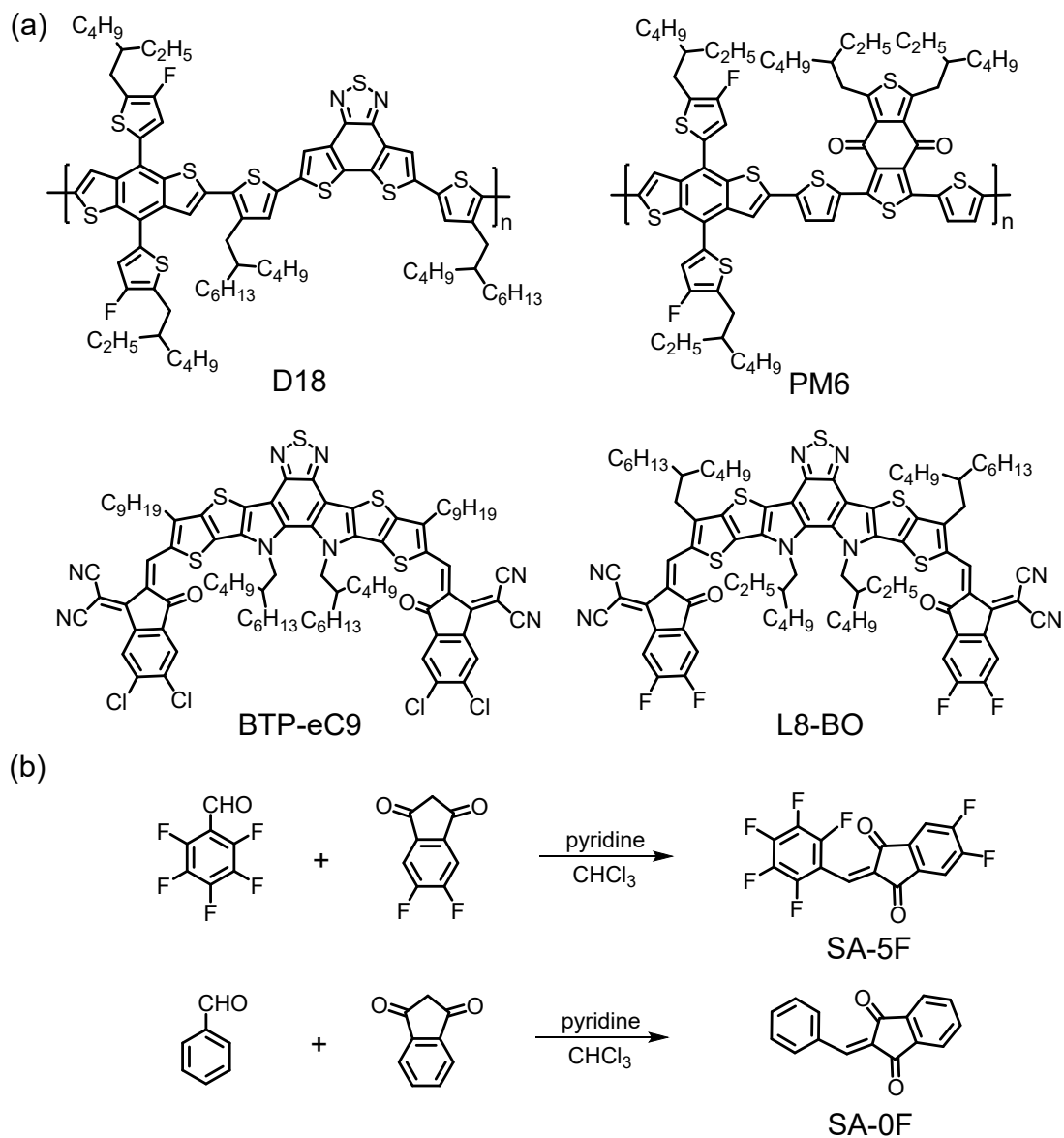


Fig. S1 (a) Chemical structures of D18, PM6, BTP-eC9 and L8-BO; (b) the synthetic route of SA-5F and SA-0F.

3. NMR spectra

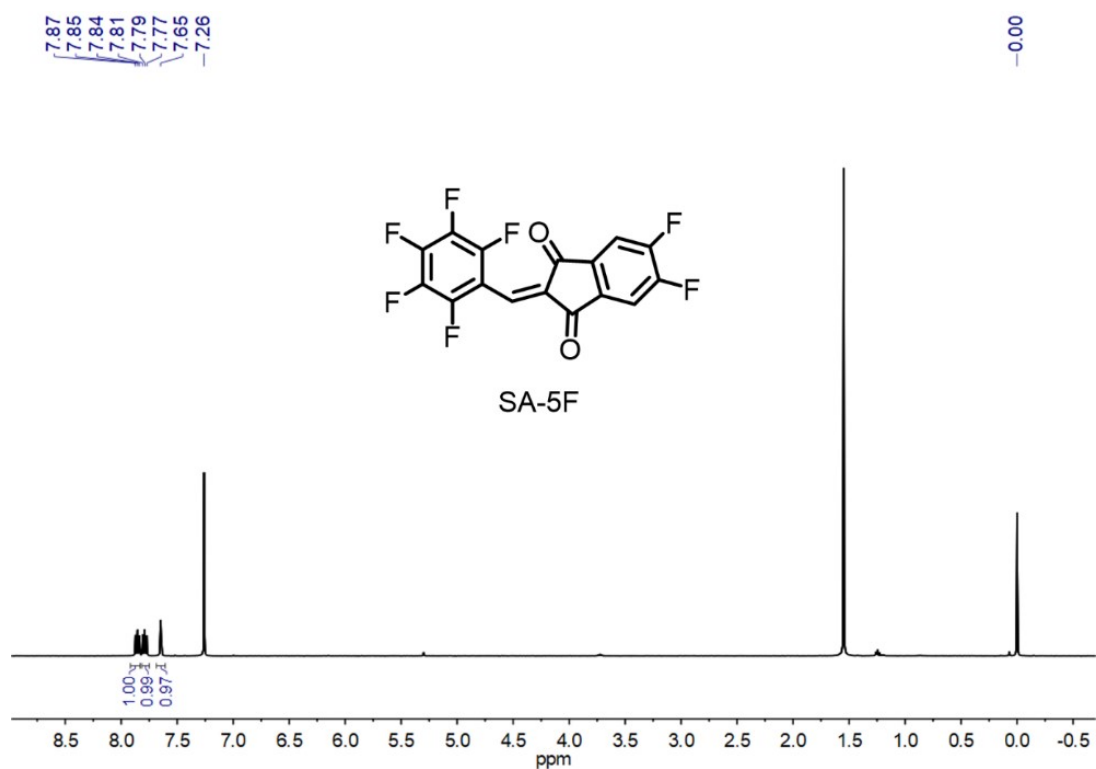


Fig. S2 ¹H NMR spectrum of SA-5F.

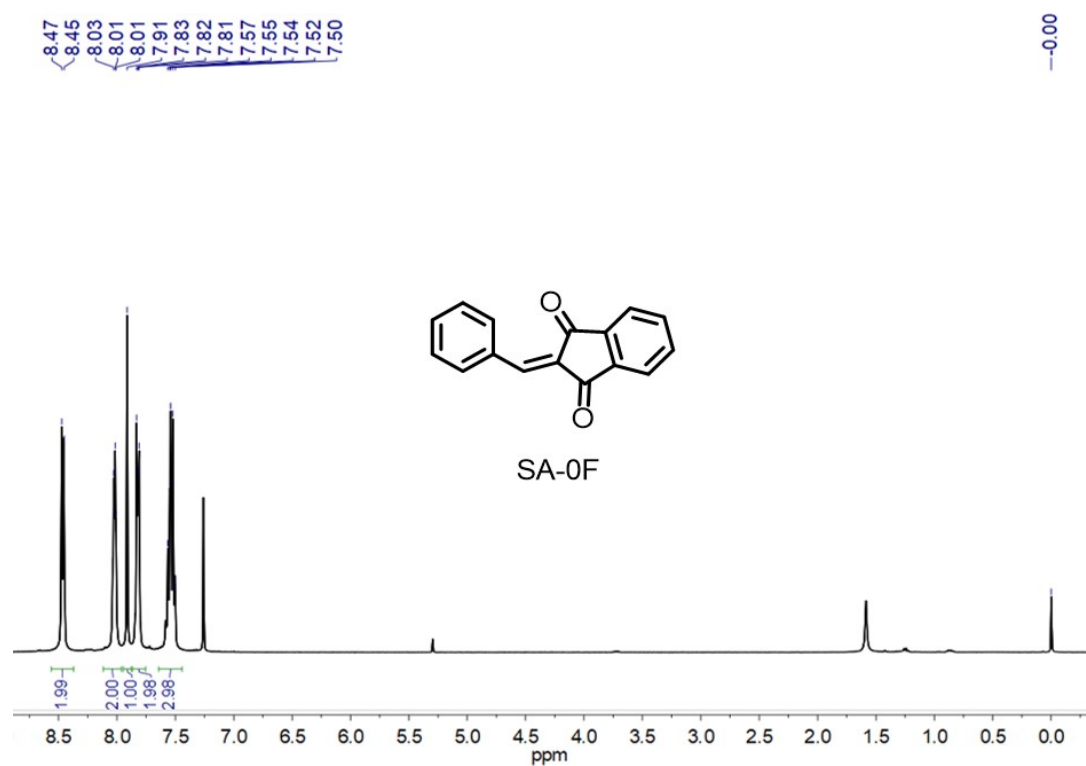


Fig. S3 ¹H NMR spectrum of SA-0F.

4. Absorption

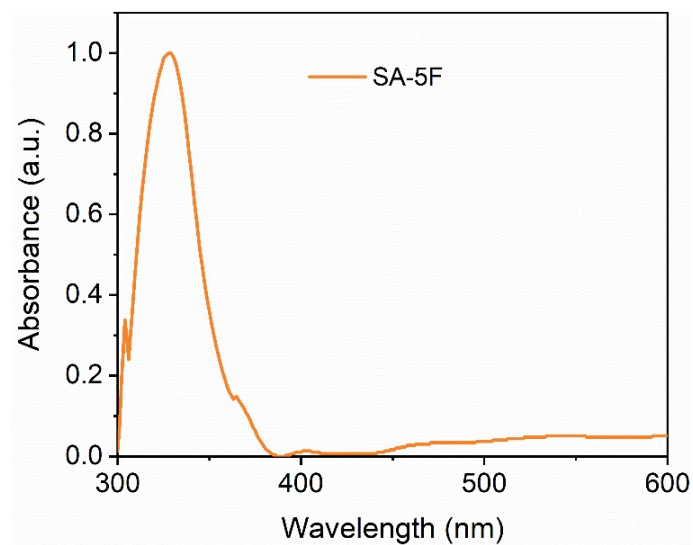


Fig. S4 UV-vis absorption spectra of polystyrene:SA-5F blend film.

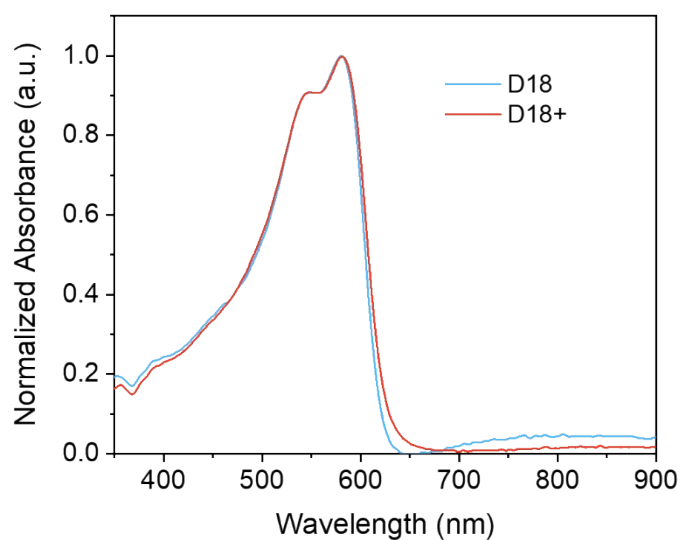


Fig. S5 UV-vis absorption spectra of D18 and D18+ neat films after thermal annealing under 80 °C.

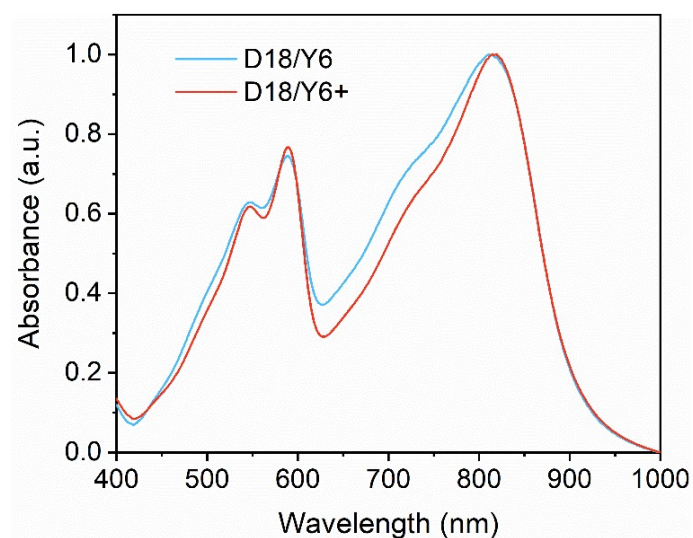


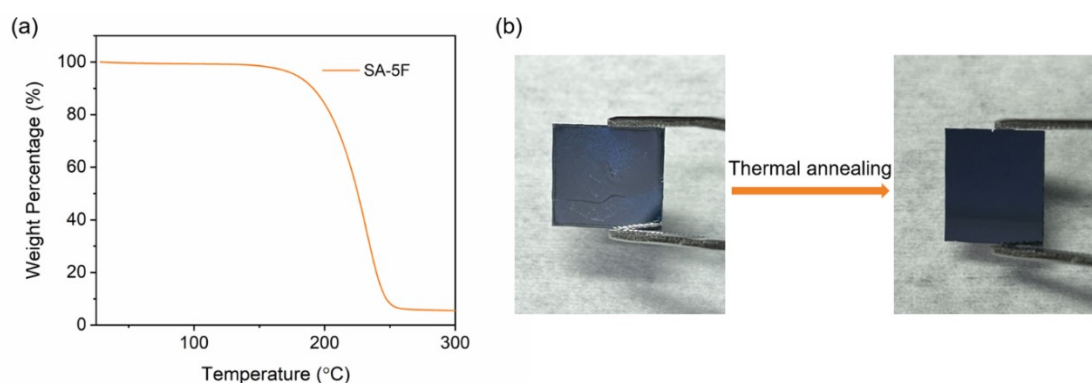
Fig. S6 UV-vis absorption spectra of D18/Y6 and D18/Y6+ PPHJ blend films.

Table S1 Optical data of Y6 and Y6+ thin films.

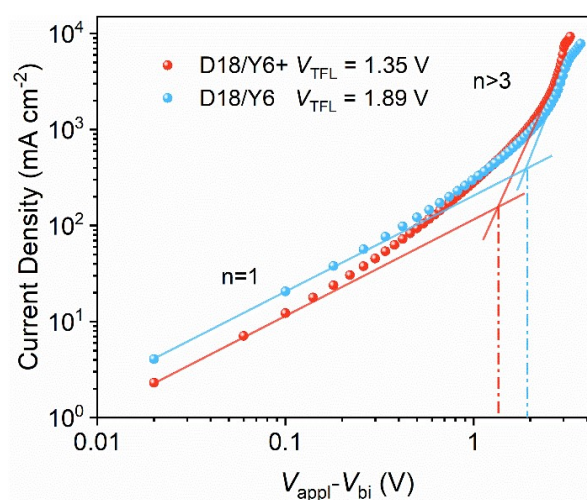
	λ_{film} [nm]	λ_{onset} [nm]	E_g^{opt} [eV]
Y6	822	919	1.35
Y6 Annealing	827	921	1.35
Y6+SA-5F	836	932	1.33
Y6+ Annealing	847	934	1.33
D18 Annealing	581	623	1.99
D18+	581	626	1.98

$$E_g^{\text{opt}} = 1240/\lambda_{\text{onset}};$$

5. TGA

**Fig. S7** (a) TGA curve of SA-5F scanned at a rate of $10.0\text{ }^\circ\text{C min}^{-1}$ under N_2 . (b) Photographs of spin-coated films of SA-5F on Si substrate before (left) and after (right) thermal annealing at $80\text{ }^\circ\text{C}$.

6. Trap density

**Fig. S8** J - V characteristics under dark for hole-only devices based on D18/Y6 and D18/Y6+ blend films (n represents the slope of the fitting line).

7. GIWAXS

Table S2 Crystal coherence length (CCL) of π - π stacking diffraction peaks and corresponding d -spacing for Y6, Y6+ neat films, and D18/Y6, D18/Y6+ PPHJ blend films.

	q_z (\AA^{-1})	d -spacing (\AA)	FWHM (\AA^{-1})	CCL (\AA)
Y6	1.76	3.57	0.309	18.30
Y6+	1.87	3.36	0.275	20.56
D18/Y6	1.71	3.67	0.287	19.70
D18/Y6+	1.86	3.38	0.253	22.35

Table S3 The lamellar stacking diffraction peaks and corresponding d -spacing for Y6, Y6+ neat films and D18/Y6, D18/Y6+ PPHJ blend films.

	q_{xy} (\AA^{-1})	d -spacing (\AA)		q_{xy} (\AA^{-1})	d -spacing (\AA)
Y6	0.29	21.66	D18/Y6	0.30	20.94
Y6+	0.32	19.63	D18/Y6+	0.33	19.04

8. AFM

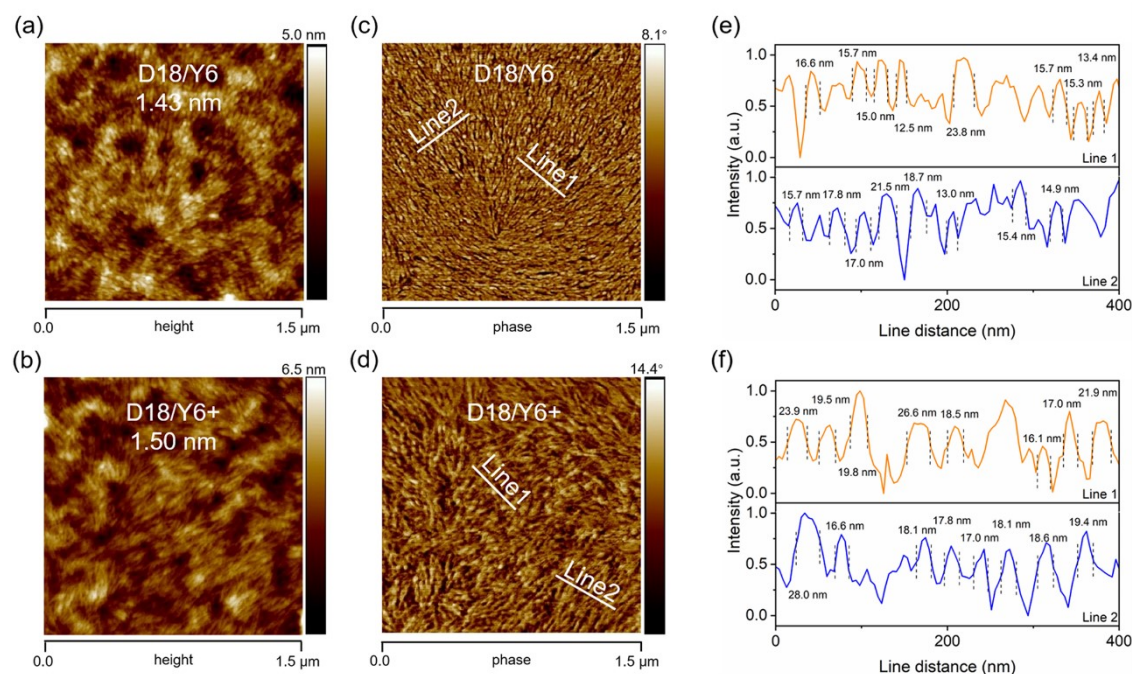


Fig. S9 AFM height images of (a) D18/Y6 and (b) D18/Y6+ PPHJ blend films, AFM phase images of (c) D18/Y6 and (d) D18/Y6+ PPHJ blend films. The line profiles along the white lines to obtain the nano-grain size of (e) D18/Y6 and (f) D18/Y6+ PPHJ blend films. The nano-grain size is obtained from FWHM (the distance between two adjacent dashed lines in the graph).

9. Theoretical calculation

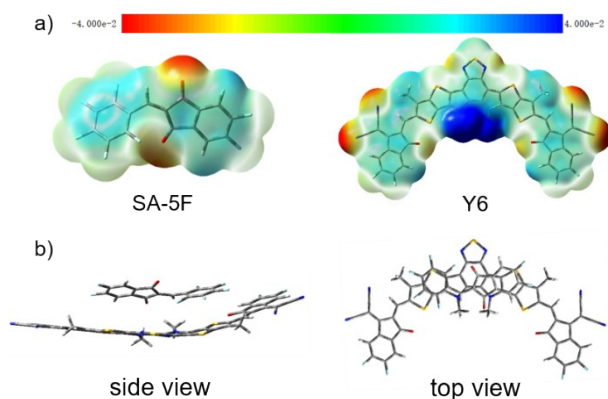


Fig. S10 a) The optimal geometry configuration and ESP of SA-5F and Y6. b) The optimal configuration of one SA-5F molecule adsorbing on one Y6 molecule.

10. TA

Femtosecond TA measurements were carried out on a homemade spectroscopy setup. The laser source is a Ti:Sa amplified laser system (25 fs, 1 kHz, 800 nm, 4 mJ/pulse, Legend Elite-1K-HE). The output pulse is split into two beams. The first beam is used to pump a tunable optical parametric amplifier (TOPAS-C, Light Conversion), which will output tunable femtosecond laser pulses from 350 nm to 2600 nm. The second beam with weaker energy is focused on an yttrium aluminum garnet plate to generate a white light continuum for the near-infrared probe. The time delay between the pump beam and the probe pulses is controlled by a motorized delay stage with a maximum delay time of 8 ns. TA spectrum was calculated from consecutive pump-on and pump-off measurements and averaged over 400 shots. All samples used TA measurements were obtained via spin-coating the solution onto the quartz substrate. The pump wavelength was set to 670 nm to excite the samples.

Table S4 The related parameters of decay dynamics for excitons.

	τ [ps]	κ [$s^{-1} \times 10^9$]	γ [$cm^3 s^{-1} \times 10^{-9}$]	D [$cm^2 s^{-1} \times 10^{-3}$]	L_D [nm]
Y6	775	1.29	2.24	0.89	8.30
Y6+	775	1.29	3.43	1.36	10.27

11. Device fabrication and measurement

The PPHJ OSC was fabricated on ITO glass with the structure of ITO/PEDOT:PSS/active layer/PDINN/Ag, where PDINN and PEDOT:PSS were used as electron-transport and hole-transport interlayers, respectively. The ITO glass substrate was cleaned by using an ultrasonic cleaner in water with detergent, deionized water, acetone, and isopropyl alcohol for 15 min successively, and subsequently treated with the ultraviolet ozone generator for 20 min. Then, the PEDOT:PSS aqueous solution was spin-coated onto the ITO substrate at 4000 rpm for 30 s, and thermal annealed under 150 °C in air for 10 min. For the active layer, the concentrations of D18 and Y6 are 3 mg mL⁻¹ and 8 mg mL⁻¹, respectively. The D18 was dissolved in chlorobenzene under 60 °C for 1h and spin-coated onto the PEDOT:PSS layer at 1000 rpm for 90 s (54±2 nm). The acceptor in chloroform without or with the solid additive, SA-5F, was spin-coated onto the top of the donor layer at 3000 rpm for 30 s, followed by thermal annealing under 80 °C for 5 min to prepare the active layer (100±2 nm for D18/Y6 PPHJ blend films and

101±2 nm for D18/Y6+ PPHJ blend films). Then, PDINN in MeOH (1 mg mL⁻¹) was deposited onto the active layer at 4000 rpm for 20 s. Finally, Ag (~100 nm) was evaporated onto the active layer under vacuum (pressure ca. 10⁻⁴ Pa). Except for the fabrication of PEDOT:PSS layer, the other processes were all carried out in a nitrogen-filled glovebox. The effective area of devices is 0.04 cm². The devices were determined with mask (The mask area is 0.0256 cm²).

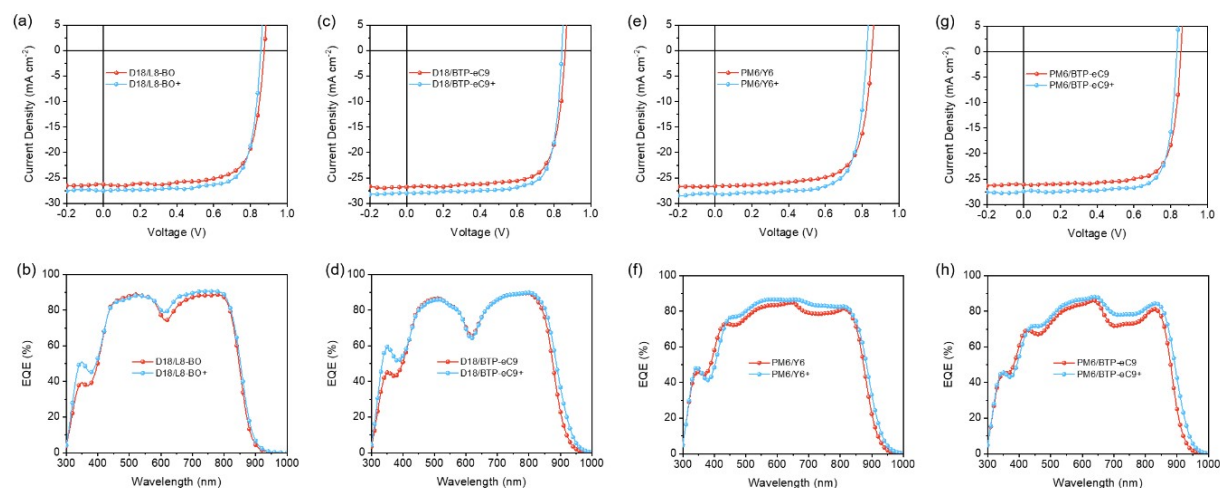


Fig. S11 *J-V* and EQE curves of PPHJ OSCs based on different donor/acceptor pairs without and with SA-5F.

Table S5 Photovoltaic parameters of PPHJ OSCs based on different donor/acceptor pairs without and with SA-5F under AM 1.5G illumination at 100 mW cm⁻². The average values and standard deviations of 10 devices are shown in parentheses.

	V_{OC} [V]	J_{SC} [mA cm ⁻²]	FF [%]	PCE [%]	J_{EQE} [mA cm ⁻²]
D18/L8-BO	0.875 (0.876±0.002)	26.29 (26.48±0.44)	73.86 (73.29±0.62)	16.99 (16.77±0.22)	25.37
D18/L8-BO+	0.856 (0.857±0.003)	27.51 (27.45±0.35)	75.88 (75.33±0.35)	17.88 (17.72±0.27)	26.17
D18/BTP-eC9	0.861 (0.860±0.003)	26.78 (26.75±0.28)	74.65 (74.35±0.61)	17.22 (17.20±0.21)	26.18
D18/BTP-eC9+	0.843 (0.843±0.003)	28.02 (27.97±0.37)	76.80 (75.71±0.47)	18.14 (17.81±0.28)	26.88
PM6/Y6	0.853 (0.854±0.002)	26.62 (26.62±0.55)	71.31 (71.02±0.44)	16.20 (16.13±0.35)	25.54
PM6/Y6+	0.825 (0.827±0.002)	28.14 (26.14±0.35)	73.80 (72.48±0.88)	17.14 (16.95±0.38)	26.77
PM6/BTP-eC9	0.855 (0.853±0.003)	26.11 (26.10±0.24)	75.90 (75.85±0.27)	16.95 (16.93±0.11)	25.04
PM6/BTP-eC9+	0.833 (0.834±0.002)	27.42 (27.46±0.25)	77.98 (76.98±0.84)	17.81 (17.69±0.25)	26.75

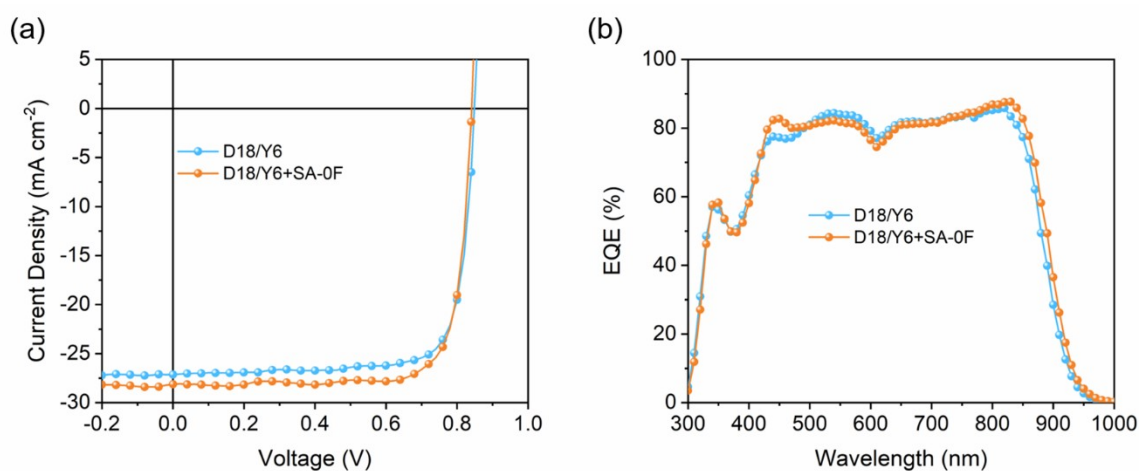


Fig. S12 J - V curves (a) and EQE spectra (b) of D18/Y6 and D18/Y6+SA-0F based PPHJ OSCs.

Table S6 Photovoltaic parameters of D18/Y6 and D18/Y6+SA-0F based PPHJ OSCs under AM 1.5G illumination at 100 mW cm⁻². The average values and standard deviations of 10 devices are shown in parentheses.

	V_{oc} [V]	J_{sc} [mA cm ⁻²]	FF [%]	PCE [%]	J_{EQE} [mA cm ⁻²]
D18/Y6	0.848 (0.847±0.002)	27.11 (27.05±0.35)	78.85 (78.02±0.77)	18.14 (17.90±0.20)	26.25
D18/Y6+ SA-0F	0.841 (0.839±0.001)	28.13 (27.91±0.23)	79.40 (79.26±0.66)	18.79 (18.56±0.40)	26.87

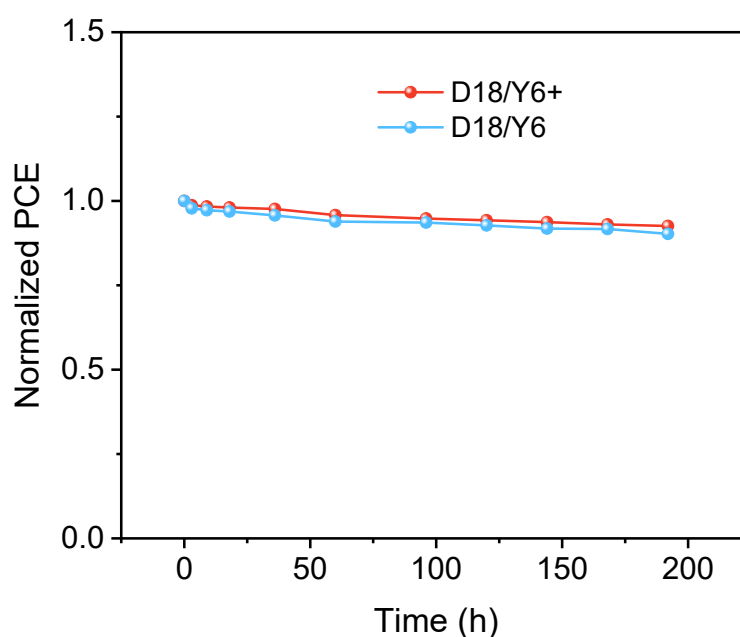


Fig. S13 Stability comparison of D18/Y6 and D18/Y6+ based PPHJ OSCs.

Electron-only devices

The structure of electron-only devices is ZnO/active layer/Ca/Al. The ZnO precursor was spin-coated onto ITO glass and annealed under 200 °C in air for 30 min. The polymer in chlorobenzene was deposited onto the ZnO layer via spin-coating with 800 rpm for 90 s, and then Y6 in chloroform was deposited onto the polymer layer via spin-coating with 3000 rpm for 30 s in the glove box under N₂. Ca (~15 nm) and Al (~60 nm) were successively evaporated onto the active layer through a shadow mask (pressure ca. 10⁻⁴ Pa).

Hole-only devices

The structure of hole-only devices is ITO/PEDOT:PSS/active layer/MoO₃/Ag. A ~30 nm thick PEDOT:PSS layer was made via spin-coating an aqueous dispersion onto the ITO glass (5000 rpm for 30 s). The PEDOT:PSS substrate was dried under 150 °C for 10 min. The polymer in chlorobenzene was deposited onto the PEDOT:PSS layer via spin-coating with 800 rpm for 90 s, and then Y6 in chloroform was deposited onto the polymer layer via spin-coating with 3000 rpm for 30 s in the glove box under N₂. Finally, MoO₃ (~3 nm) and Ag (~100 nm) were successively evaporated onto the active layer under a shadow mask (pressure ca. 10⁻⁴ Pa).

12. SCLC

Charge carrier mobility was obtained by using the SCLC method. The mobility was determined by fitting the dark current to the model of a single carrier SCLC, which can be described as:

$$J = \frac{9}{8} \varepsilon_0 \varepsilon_r \mu \frac{V^2}{d^3}$$

where J is the current density, μ is the zero-field mobility of electron (μ_e) or hole (μ_h), ε_0 is the permittivity of the vacuum, ε_r is the relative permittivity of the material, d is the thickness of the blend film, and V is the effective voltage, $V = V_{\text{appl}} - V_{\text{bi}}$, where V_{appl} is the applied voltage, and V_{bi} is the built-in potential determined by the electrode work function difference.

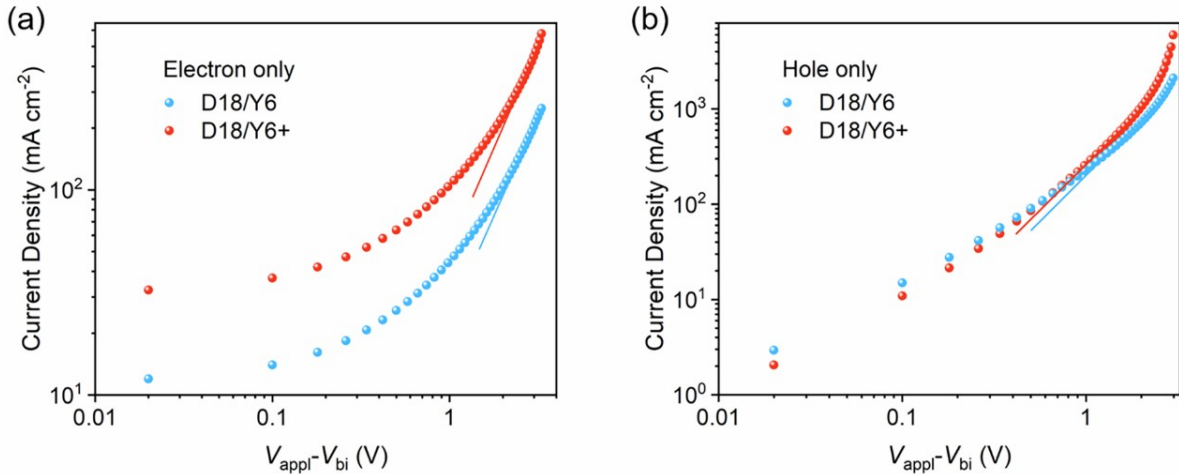


Fig. S14 Typical current density-applied voltage semi-log plots for electron-only devices (a) and hole-only devices (b) based on D18/Y6 and D18/Y6+ PPHJ blend films under dark. Measured data are shown as symbols, while the solid lines are the best fits to the SCLC model. Mobilities were extracted from the fitting.

Table S7 Charge carrier mobilities of devices based on D18 /Y6 and D18/Y6+ PPHJ blend films.

	μ_h ($10^{-4} \text{ cm}^2 \text{ V}^{-1} \text{ s}^{-1}$)	μ_e ($10^{-4} \text{ cm}^2 \text{ V}^{-1} \text{ s}^{-1}$)	μ_h/μ_e
D18/Y6	6.09	1.01	6.0
D18/Y6+	8.41	2.16	3.8

References

- [1] R. Yu, H. Yao, L. Hong, Y. Qin, J. Zhu, Y. Cui, S. Li, J. Hou, *Nat. Commun.* **2018**, *9*, 4645.